JOURNAL OF MATERIALS SCIENCE 37 (2002) 649–654

Influence of the thermal-spray procedure on the properties of a nickel-chromium coating

V. HIGUERA, F. J. BELZUNCE, A. CARRILES, S. POVEDA
Universidad de Oviedo. Campus Universitario. 33203 Gijón. Spain
E-mail: belzunce@etsiig.uniovi.es

A modified NiCr coating was thermal-spray projected using different procedures (flame, plasma, HVOF and HFPD) onto stainless steel specimens. This type of coating is normally used as protection against heat, corrosion and erosion actions encountered in superheater and reheater tubes in power plant boilers. The microstructures, porosities, oxide contents and microhardnesses of the coatings were determined. Thermal fatigue tests under an atmosphere similar to power plant service conditions were conducted in an experimental combustion chamber and, finally, the adhesion between the substrate and the coating layer was evaluated by means of tensile tests. The results obtained are discussed, with special attention being paid to the specific characteristics of the different spraying procedures.

1. Introduction

The development of corrosion and erosion protection elements for superheater and reheater tubes in power plant boilers using thermal-spray techniques requires in-depth knowledge of the principal characteristics of these products and careful evaluation of their service performance [1]. There are currently not only a great variety of materials available but also a number of different commercial thermal-spray procedures, some of which have been only recently developed, which are assumed to function effectively in this specific application. The same can also be said of many other technical applications, since the use of these surface protection procedures is increasing at a high rate. The aim of the present study is to analyse the influence of thermal-spray procedures on the final characteristics of the coatings obtained using different commercially available thermal-spray methods.

2. Thermal-spray processes

Thermal-spray processing is a very rapidly expanding field of surface engineering. In all thermal-spraying processes, the consumable coating material fed to the spray gun is raised in temperature and projected at a high velocity against the workpiece, where the individual hot particles form splats that interlock and gradually build up a coating of the desired thickness. The main differences between the available procedures are the energy source involved and the type of gun used in the projection [2].

Flame spraying is a low-energy process. It uses a combustible gas as a heat source to melt the coating material. Most flame spray guns can be adapted to use several combinations of gases, such as acetylene, propane, hydrogen, etc., together with oxygen. Flame temperatures depend on the oxygen-to-fuel ratio and pressure, which ranges between 2,500–3,000 K. The maximum particle velocity is also much lower than that attained in high-energy processes (below 100 m/s) [3].

High velocity oxyfuel (HVOF) is a high-energy process. It has specially designed spray guns that burn oxygen and a fuel gas (hydrogen, propane or propylene). In HVOF systems, the combustion process takes place within the gun, and the gas flow rates are much higher than in conventional flame spraying. The combination of these two factors leads to supersonic flame speeds, up to approximately 2,000 m/s, with particle velocities that may reach 800 m/s. The maximum temperature attained in these processes is only slightly higher than in normal flame spraying [2, 4].

Plasma spraying is a high-energy process in which a high current arc is generated within the torch and a gas is injected into the arc chamber, where it is heated and converted into a high temperature plasma. In practice, pure argon or nitrogen is used as the primary plasma gas, together with additions of 2–25% of a secondary gas (hydrogen or helium). Powdered surfacing material is injected into this plasma jet and is hence heated to a molten state and accelerated onto the substrate. Plasma temperatures higher than 10,000 K and particle velocities of up to 600 m/s have been measured in some specific cases [5].

The high frequency pulse detonation (HFPD) spray process is based on a carefully designed gun capable of producing discontinuous behaviour (cycled explosions) from a continuous supply of the detonable gases and powders. The system allows the self-generation of discrete batches of gases and powders for each cycle, opening up the possibility of working in a wide range of explosion frequencies (up to more than 100 Hz) and gas mixtures. In the HFPD process, the flow of gaseous

products from cycled explosions in the gun is used to accelerate and heat the sprayed particles. Typically, these particles attain very high speeds (up to 800 m/s) and moderately high temperatures (in the order of 4,000 K) leading to quite dense, well-bonded coatings of most commercially available powders (metallic alloys, ceramics and cermets) [6]. One of the most important consequences of the particular physical process involved in HFPD cycled explosions is the low consumption of gases, especially when compared with alternative continuous HVOF systems.

3. Experimental procedure

3.1. Materials

An AISI 304 austenitic stainless steel in a fully annealed condition was used as substrate. All the specimens used in the experiments were cylindrical, with a diameter of 25.4 mm and a length of 25.4 mm, in agreement with the ASTM C633 standard [7], and were obtained through calibrated profiles.

Table I lists the composition and granulometry of the commercial alloy powders that were thermally sprayed according to the different projection procedures. This modified NiCr alloy is usually employed as a high temperature corrosion resistant coating in boilers. A bonding coat (NiMoAl) was used in the case of the flame-sprayed projection in order to improve the substrate-coating adherence of the method.

3.2. Projection procedures

Firstly, the stainless steel substrates were grit blasted according to the procedures described in Table II, where the final roughness after grit blasting is also presented.

TABLE I Composition of coating materials

Element:	%Cr	%Ni	%Ti	%Al	%Mo
Coating	47.5	51.0	0.52	0.23	–
Bonding coat:					
Coating type A2	–	balance	–	6.5	6.0

TABLE II Grit blasting procedures

Grit blasting	Flame	Plasma	HVOF	HFPD
Abrasive	Angular steel	Angular steel	Alumina	Alumina
Air pressure (MPa)	1	1	0.5	0.7
Roughness, Ra (μm)	12.9	12.9	3.2	4.8

The modified NiCr coating was thermally sprayed onto the stainless steel substrates by means of flame (A1, A2), plasma (A3), high velocity oxygen fuel, HVOF (A4) and high frequency pulse detonation, HFPD (A5) procedures. Table III shows the different combinations of coatings and projection methods mentioned above.

METCO plasma-spray and flame-spray utilities were used to project the powders onto the substrates. The apparatuses used to carry out the HVOF and HFPD projections were a CDS-100 from Plasma Technik and a PK200 Aerostar Coatings, respectively. The most relevant projection parameters are listed in Table IV.

Samples were cleaned, grit blasted and coated with the nickel-chromium alloy within the 2 hours following cleaning. An automatic device was used to minimize fluctuation of the spray parameters in order to achieve coatings of homogeneous thickness.

3.3. Characterising tests

The thickness of the coatings, along with their microstructure, porosity and oxide content, were determined by means of optical microscopy techniques. Coating porosity and volume fraction of oxides were evaluated according to the ASTM E562 standard [8] by point counting on different fields. Vickers microhardness tests using 200 g load were also performed in order to assess the coating hardness and substrate plastic strain hardening promoted by the high speed projection.

Thermal fatigue experimental tests were carried out in a 210 kW laboratory combustion unit ($Q = 780{,}000$ kJ/h) using methane as fuel. The combustion atmosphere composition was approximately the same as that usually existing in actual power plants with a free oxygen volume per cent of 3–3.5%. The cyclic thermal fatigue tests were carried out by means of repeating the following cycle five times: a heating period of one hour to reach 800°C (1,073 K), followed by another hour for cooling to 100°C (373 K, $\Delta T_{avg} = 12$ K/min).

Adherence tests were also performed in accordance with the ASTM C633 standard [7] in order to assess the quality of the substrate-coating bonding and the influence of cyclic thermal fatigue on the aforementioned adherence. Finally, these samples were sectioned perpendicular to their surface, ground, polished and analysed under optical and scanning electron microscopes.

TABLE III Coating materials and thermal-sprayed methods

Coatings:	A1	A2	A3	A4	A5
Powders	NiCrAlTi	NiCrAlTi	NiCrAlTi	NiCrAlTi	NiCrAlTi
Granulometry, μm	44–88	44–88	44–88	44–88	44–88
Thermal spraying:	Flame	Flame	Plasma	HVOF[a]	HFPD[b]
Coatings thickness, μm	540–560	425–450	440–454	418–425	452–459
Bonding coat powder:	–	NiMoAl	–	–	–
Granulometry, μm		44–105			
Bonding coat thickness, μm	–	100–110 μm	–	–	–

[a]HVOF - High velocity oxygen fuel.
[b]HFPD - High frequency pulse detonation.

TABLE IV Flame and plasma spraying parameters

Spray method:	Flame	Flame bonding coat	Plasma	HVOF	HFPD
Frequency:					50 Hz
Arc power:			600 A; 60–70 V		
Carrier gas:			Nitrogen	Nitrogen	Nitrogen
Projection distance, mm	150	125	120	300	200
Plasmogen gas and pressure (MPa)			Nitrogen, 0.52		
Fuel:	Acetylene	Acetylene		Propylene	Propylene
Fuel flow:	0.96 m^3/h	0.93 m^3/h		80 1/min	45 1/min
Oxygen flow:	1.7 m^3/h	1.3 m^3/h		400 1/min	170 1/min

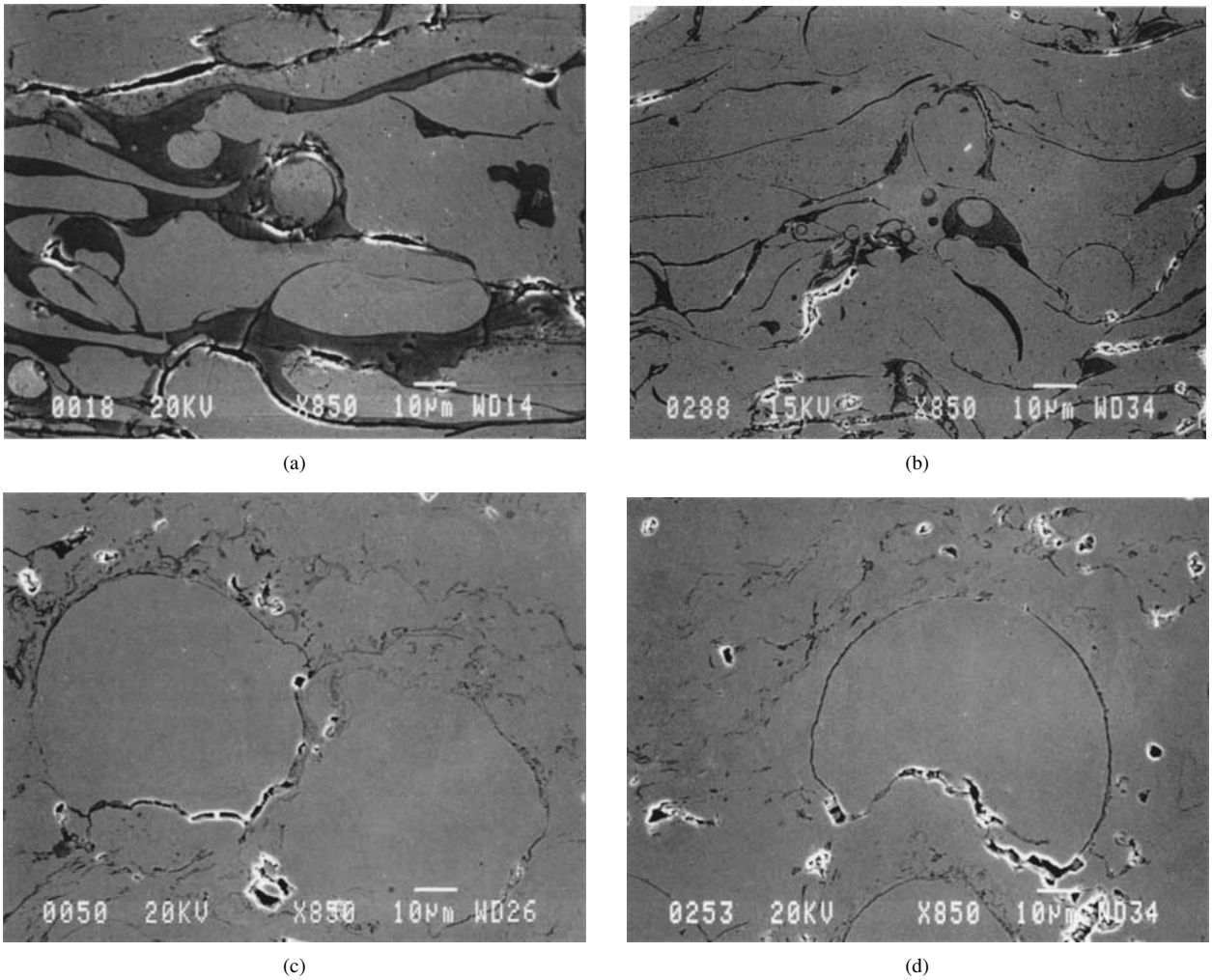

(a) (b) (c) (d)

Figure 1 Coatings microstructure. a) NiCr flame spray coating, b) NiCr plasma spray coating, c) NiCr HVOF coating, d) NiCr HFPD coating.

4. Results

4.1. Microstructure and microhardness

Fig. 1 shows the typical cross-sectional microstructures corresponding to the four coatings obtained by means of the different spray-coating procedures.

Table V shows the average microhardness of the coatings, along with their porosity and volume fraction of oxides. The dependence of porosity and oxide content on the spray procedure can be clearly seen. The oxide content depends on the temperature and contact time with air during spraying; the high velocity and low temperature of the HFPD procedure thus explains the lowest value obtained in this case. The very high temperature of plasma spraying and the low velocity of flame spraying (long interaction time) justify the high oxide contents reported in these two procedures. On the other hand, the porosity obtained after plasma-spraying and HVOF procedures was the lowest, while the characteristic low temperature of HFPD reduces the final cohesion of this coating. It must also be stressed that many powder particles were not melted when the HFPD-sprayed application method was used and this fact can be identified in the coating microstructure as rounded particles (the same occurs with the HVOF method, though not so consistently, Fig. 1c and d). The very low impact speed, typical of flame spraying,

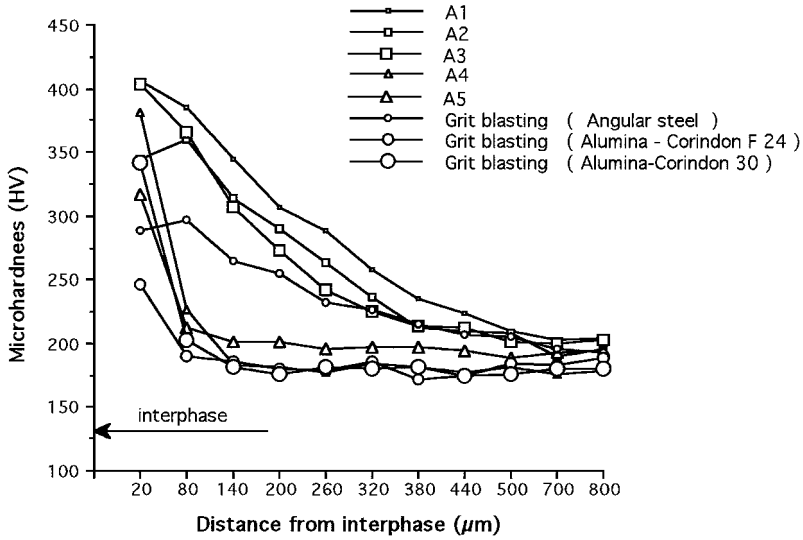

Figure 2 As-sprayed substrate microhardness profiles. Distances are measured from the coating-substrate interface.

TABLE V Coating microhardness, porosity and volume fraction of oxides

Coatings:	A2	A3	A4	A5
Microhardness (HV)	301	284	298	303
Porosity (% vol. avg.)	5	1	0.7	1.75
Oxide Content (% vol. avg.)	17	5.2	3.6	2.1

justifies the high porosity of this last procedure. Incidentally, the coating hardness does not depend significantly on the spraying procedure.

Fig. 2 shows the clear hardening of the substrate surface due to the high-speed impact of the projected particles during projection: hardness values greater than 400 HV were measured on the substrate region closer to the coating, while the average substrate hardness was around 200 HV. The hardness profile of the grit blasted substrates can also be seen as a reference.

The most distinctive difference between the spraying methods is the length of the hardened region, which is smaller in HVOF and HFPD procedures (0.15 versus 0.5 mm). This latter fact may be attributed to the prior effect of grit blasting, as can be seen when comparing the prior hardening due to grit blasting with the final hardening, which is the consequence of both procedures, grit blasting and thermal spraying. The different grit blasting methods, described in Table II, modify substrates differently: along with a substantial increase in roughness (see Table II), a clear higher degree of hardness and a larger affected zone are obtained when the grit blasting air pressure is increased. Finally, the hardening effect due to thermal spraying exclusively affects a substrate region of approximately 100 μm measured from the substrate-coating interface, while deeper hardening is due to grit blasting. Fig. 3 shows the slip bands produced by intense plastic deformation, which takes place in the strain hardened region existing just below the coating.

Maintaining the coated materials at low temperatures does not modify the hardness of the aforementioned region. However, recrystallization processes take place at higher temperatures and its hardness clearly decreases. Recrystallization phenomena, as can be deduced from the data presented in Fig. 4, are produced when heat-treated at 800°C (1,073 K). According to [9], austenitic stainless steels begin to recrystallize around 700°C (973 K).

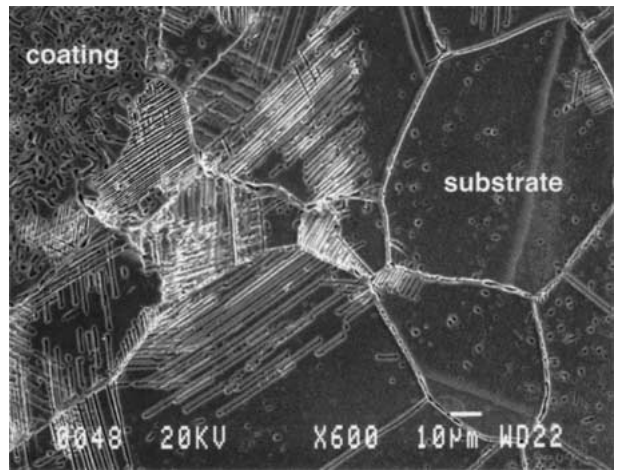

Figure 3 Slip bands in the substrate region near the substrate-coating interface.

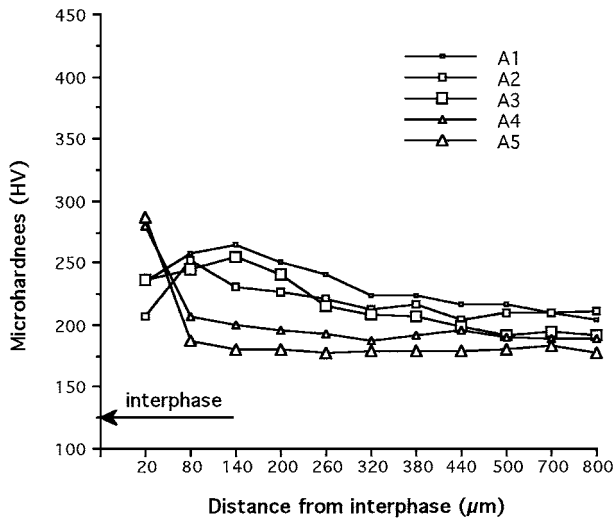

Figure 4 Substrate microhardness profiles after 800°C (1073 K) testing. Distances are measured from the coating-substrate interface.

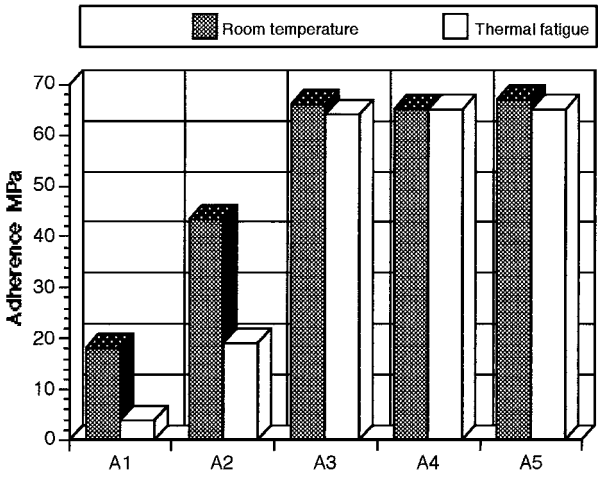

Figure 5 Adherence values in the as-sprayed and after thermal fatigue conditions.

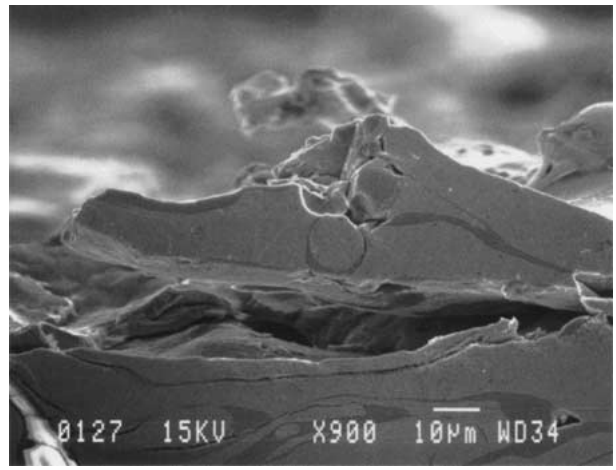

Figure 6 Cohesive coating fracture. NiCr flame spray coating.

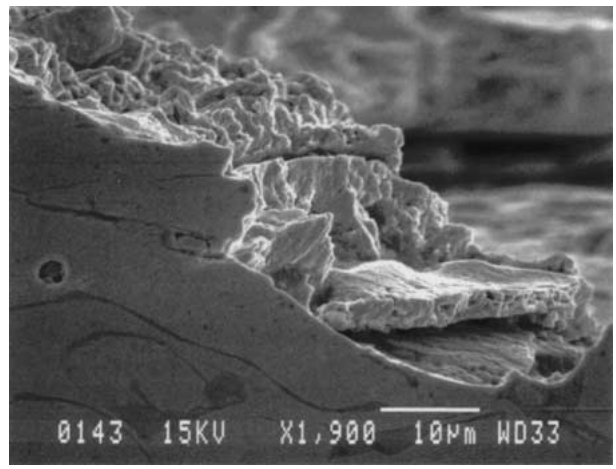

Figure 7 Cohesive fracture of NiCr plasma spray coating.

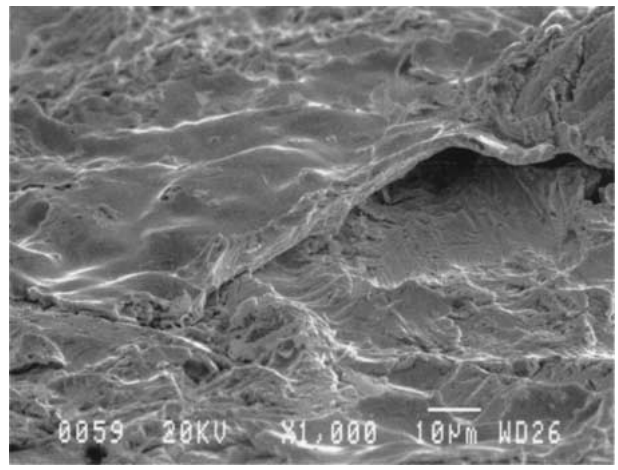

Figure 8 Adhesive failure of HVOF NiCr coating. Grit blasted substrate is seen in the lower right corner.

4.2. Coating adherence

Initial tensile adherence strengths of the coating-substrate interface measured at room temperature after flame- and plasma-spray, HVOF and HFPD projections are presented in Fig. 5. The adherence strengths of the same materials after the thermal fatigue tests are also presented in said Fig. 5.

Average adherence values at room temperature are in the range of 20 MPa for the modified NiCr flame-sprayed coatings, and increase to about 40 MPa when a bonding layer is applied. When the modified NiCr coating is applied by means of the plasma-spray method, HVOF or HFPD, the room temperature adherence increases to values higher than 60 MPa.

Under thermal fatigue conditions, the adherence of the flame-sprayed modified NiCr coating (A1) clearly decreases to very low values, the same also occurring when a bonding coat is employed (in this case the residual adherence value is below 20 MPa). All the other coatings (plasma-sprayed, HVOF and HFPD) maintain their adherence after thermal fatigue testing without any significant change.

After detailed examination of the adherence pattern of the as-sprayed materials under the scanning electron microscope, it can be concluded that flame-sprayed (with a bonding layer) and plasma-sprayed coatings fracture was always cohesive and took place preferentially through the internal porosity and the oxide layers formed during the spray operation, as can be seen in Figs 6 and 7 [10]. In all cases, the coating fracture was brittle and no sign of plastification was observed. These figures clearly show the typical layered fracture surface as the tensile load is applied perpendicular to the layered coating structure: the flattened metallic particles debond through their oxide interfaces (most of which are chromium oxides). The elongated appearance of these hard, brittle oxides (Fig. 1) promotes high stress concentration, crack nucleation and sudden growth. At the same time, the much lower adherence values obtained with flame-sprayed coatings can now be justified by their larger oxide volume fraction. In contrast, adhesive failure was observed in the case of flame-sprayed coatings projected without a bonding layer and in HVOF and HFPD coatings, although in these cases under a much higher adherence value, as can be seen is Fig. 5. Fig. 8 shows the interface between substrate and coating in the case of the HVOF coating after adherence testing and Fig. 9 shows a small, residual piece of coating in the failure due to adherence loss in the HFPD coating.

Exposure to thermal fatigue does not modify the coating fracture pattern and its more relevant effects

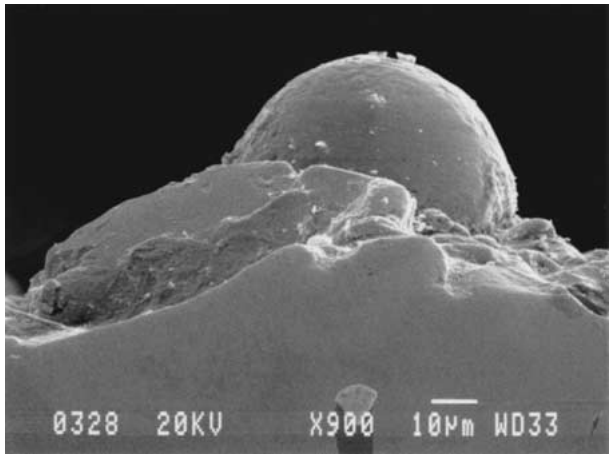

Figure 9 Adhesive failure of HFPD NiCr coating. Residual piece of coating onto the substrate.

in flame-sprayed coatings must be justified on the basis of thermal stresses generated in the internal metal-oxide and coating-substrate interfaces (due to differences in thermal expansion of both phases).

5. Conclusions

Thermal-sprayed processes used to obtain anti-wear coatings, applied after prior grit blasting of the substrate surface, produce an increased subsurface hardening of the stainless steel substrate which is characterized by the presence of slip bands and which affects a region of approximately 100 μm. When these coatings are submitted to high temperature conditions, recrystallization processes take place and the hardness of this region decreases considerably. The microstructure of the coating (porosity and oxide volume fraction) depends on the projection method. The oxide content depends on both the maximum temperature attained and the interaction time between powders and air that occurs during the spraying fly. Porosity is also related to the spraying procedure by means of the average temperature and velocity attained by the particles when they impact with the cold substrate.

The substrate-coating adherence of the high energy spray procedures (plasma, HVOF and HFPD) are very high and are not affected by thermal fatigue, this property being limited by the presence of brittle oxides in the case of plasma projection and by the substrate-coating interface in the other two cases. The adherence of flame spraying is much lower, and hence a bonding layer has to be necessarily applied between substrate and coating.

Acknowledgement

This study was subsidized by FICYT (Principado de Asturias), Project number PC-MAT 98-01.

References

1. AMERICAN WELDING SOCIETY, "Thermal Spraying" (American Welding Society, 1985) p. 6.
2. S. GRAINGER and J. BLUNT, "Engineering Coatings" (Abington Publishings, 1998) p. 119.
3. H. HERMAN and S. SAMPATH, "Metallurgical and Ceramic Protective Coatings" (Chapman & Hall, 1996) p. 261.
4. J. M. GUILLEMANY and J. SANCHEZ, *Tratamientos Térmicos* (1997) 36.
5. R. C. TUCKER, "Surface Engineering," ASM Handbook, Vol. 5 (ASM International, 1994) p. 497.
6. I. FAGOAGA, G. BARYKIN, J. DEJUAN, T. SOROA and C. VAQUERO, in Proceedings of the United Thermal Spray Conference, Düsseldorf, Germany, 1999, edited by DVS-Verlag, p. 282.
7. ASTM C 633, ASTM Standards (1979).
8. ASTM E 562, ASTM Standards (1976).
9. American society for metals, "ASM Handbook," Vol. 1 (ASM International, 1990) p. 841.
10. V. HIGUERA, F. J. BELZUNCE and E. FERNANDEZ, *Tribology International* **30** (1997) p. 641.

Received 14 June 2000
and accepted 3 August 2001